

Theoretical study of hydrogen bonding interactions on MDI-based polyurethane

Cuili Zhang · Jinlian Hu · Shaojun Chen · Fenglong Ji

Received: 1 November 2009 / Accepted: 19 December 2009 / Published online: 16 February 2010
© Springer-Verlag 2010

Abstract Hydrogen bonding among hard–hard segments and hard–soft segments in 4,4'-diphenylmethane diisocyanate (MDI)-based polyurethane was investigated theoretically by density functional theory (DFT). Both B3LYP/6-31G* and B3PW91/6-31G* methods gave good structures, reasonable Mulliken charges, binding energies, dipole moments, and good infrared (IR) spectra trends in predicting hydrogen bonding. Bond distances $R(\text{N}-\text{H}\cdots\text{O})$, which were in the range of 3.005–3.028 Å for the carbonyl bonded hydrogen-bond, and 3.074–3.075 Å for the ester bonded hydrogen-bond, are in reasonable agreement with experimental values. Most of the carbonyl oxygen in polyurethane exists in a hydrogen-bonded form. Complex (c), with two carbonyl hydrogen bonds, features the largest dipole moment, while complex (d) with two ester hydrogen bonds, possesses the smallest dipole moment, i.e., lower than that of the isolated monomer, which may be due to the symmetry of the two monomers. These results confirm that the DFT method is a good tool with which to study weak interactions, and indicate that hydrogen bonds are indeed formed between carbonyl and N-H, or ester and N-H, with the former being stronger.

Keywords Hydrogen bonding · Density functional theory · 4,4'-diphenylmethane diisocyanate · Interaction

Introduction

Shape-memory polymers can recover their original shape by being heated above their transition temperature, which is defined by the different phases in the materials. In particular, the shape-memory properties of segmented polyurethane block copolymers (PU) have been extensively researched because of its superior material properties, which arise from the phase-separated structure of its hard and soft segments. The hard segments, which are based on diisocyanate and diamine, form physical crosslinks arising from polar interactions, hydrogen bonding, and crystallization in the hard domain; while the soft segments are typically polyether blocks, and form the reversible phase because of molecular motion in a rubbery state. The compound 4,4'-diphenylmethane diisocyanate (MDI) is one of the most widely used hard-segment-determining raw materials in polyurethane synthesis [1–5]. A simple MDI-based polyurethane interaction model was built including the hard segment (diphenylmethane diisocyanate part) and soft segment (ether oxygen part; Fig. 1).

A hydrogen bond (H-bond) forms due to the attractive force between the hydrogen attached to an electronegative atom of one molecule and an electronegative atom of a different molecule, which is really a special case of dipole forces. Hydrogen bonding significantly affects the physical properties of the hard segments in polyurethane; binding of the hard segments makes the PU very solid below its melting temperature. Hydrogen bonding in polyurethanes has been extensively studied using infrared (IR) spectroscopy [6–12], and is evidenced by a frequency shift to

C. Zhang · J. Hu (✉) · S. Chen · F. Ji
Institute of Textiles and Clothing,
The Hong Kong Polytechnic University,
Hung Hom, Hong Kong, China
e-mail: tchujl@inet.polyu.edu.hk

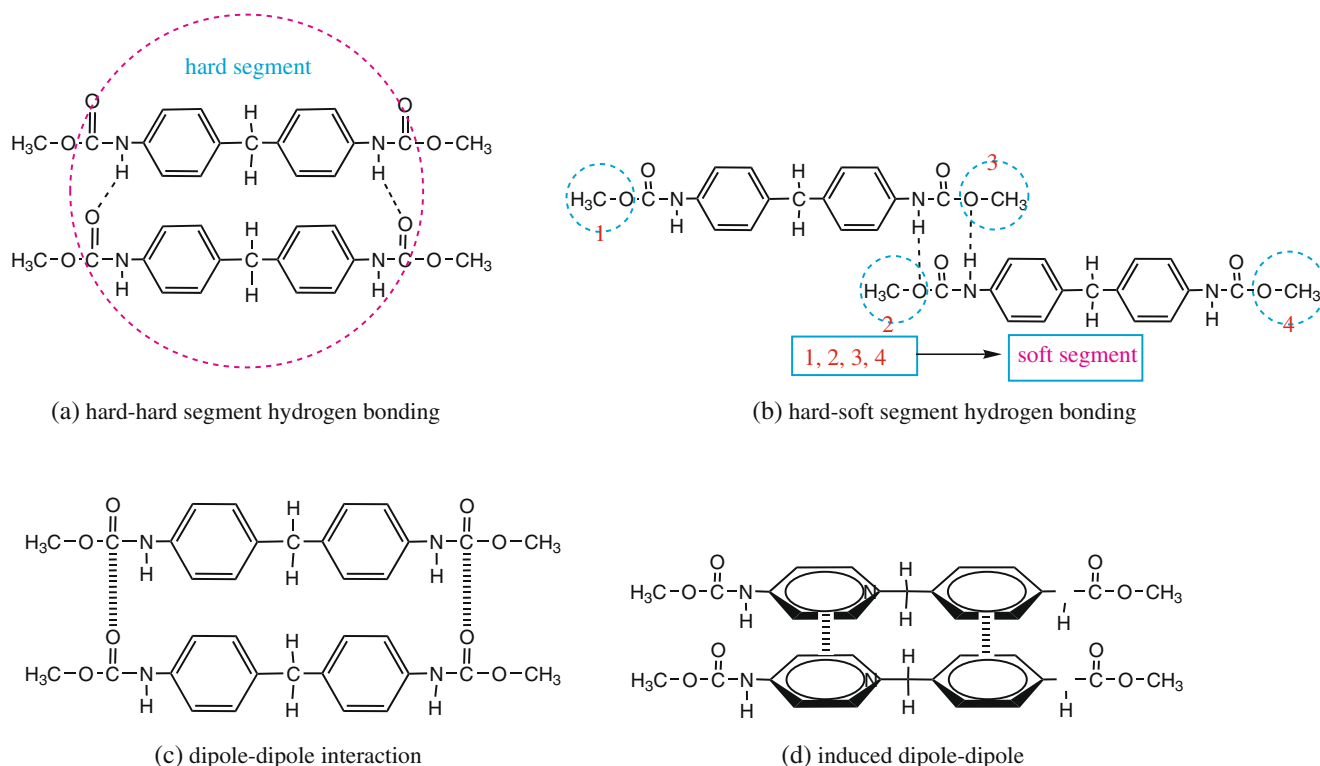


Fig. 1 Possible interactions in 4,4'-diphenylmethane diisocyanate (MDI)-based polyurethane

values lower than those observed when these groups are free (i.e., not hydrogen bonded). The magnitude of the frequency shift is a measure of hydrogen bond strength. In polyether-based polyurethanes, the fraction of hydrogen-bonded carbonyls, as characterized by a hard-hard segment hydrogen bond ($\text{N-H}\cdots\text{O}=\text{C}$; Fig. 1a), was used as a measure of the extent of phase separation. The N-H group could also form a hard-soft segment hydrogen bond with the ether oxygen ($\text{N-H}\cdots\text{O}$; Fig. 1b), which represents the extent of phase mixing between hard and soft segments. Lee [2] pointed out there are three kinds of interactions among polyurethane chains that are responsible for the shift in the transmittance peak with the inclusion of more hard segment: (1) hydrogen bonding between the carbamoyl and carbonyl groups of the hard segment; (2) dipole-dipole interactions between carbonyl groups of hard segments; (3) induced dipole-dipole interaction between aromatic rings of hard segments (Fig. 1a,c,d).

However, to the best of our knowledge, theoretical studies on the bonding mechanism of the hard-hard and hard-soft segments in polyurethane are still very rare, while those on hydrogen-bonded complexes have been an active area of research for the past several years [13]. Here, we investigate interactions in the MDI-based polyurethane shown in Fig. 1 by density functional theory (DFT) using B3LYP and B3PW91 methods and the 6-31G* basis set. The results provide valuable insight into phase separation and phase mixing in polyurethanes.

Computational methods

The Hartree-Fock (HF) method neglects electron correlation, which results in an overestimation of bond lengths [14], while DFT-based methods, such as the Becke-three Lee-Yang-Parr (B3LYP) [15] method, have been shown to provide reliable trends of binding energies even though the small energy differences often observed in relative binding energies can be overshadowed by the DFT quadrature errors [14]. Different functionals were used in the DFT calculations. The Becke exchange functional [16], containing the gradient correction and denoted by B, was combined with correlation functionals by Lee, Yang, and Parr (LYP) [17] and by Perdew and Wang (PW91) [18], which results in BLYP and BPW91 exchange-correlation functionals. The hybrid method suggested by Becke [15], which includes a mixture of the HF component and the DFT exchange-correlation functional, is denoted by B3LYP and B3PW91.

In this work, the equilibrium geometries, interaction energies, binding entropies, Mulliken charges, dipole moments and IR spectra were calculated by both B3LYP and B3PW91 methods using the 6-31G* basis sets. The obtained binding energies of the complexes were corrected both for basis set superposition error (BSSE) by the Boys-Bernardi full counterpoise method [19], and for zero-point vibrational energy (ZPE) at 298.15 K. Harmonic frequency analyses have been carried out and all the optimized geometries have no imaginary frequency, which suggests

that the optimized structure exists in the minimum state. It is well known that vibrational frequencies obtained by quantum chemical calculations are typically larger than their experimental counterparts. Therefore, to compare the calculated vibrational frequencies with experimental values, the former were scaled by 0.9603 for B3LYP/6–31G* and 0.9567 for the B3PW91/6–31G*, respectively. All calculations were performed with the Gaussian 03 program [20].

Results and discussion

We calculated three types of H-bonds, represented by complexes (b), (c) and (d) in Fig. 2, at both B3LYP/6–31G* and B3PW91/6–31G* levels. The corresponding geometry parameters are listed in Table 1. Table 2 shows

the Mulliken charges at key points of the hydrogen bonding. Harmonic frequency analyses indicate that the obtained structures are true minima. The hydrogen-binding energies (including BSSE and ZPE corrections) and binding entropies are listed in Table 3. Figure 3 and Table 4 show the IR spectra and dipole moments, respectively. The following sections discuss these interactions in detail.

Geometry structures

Hydrogen bonds can form between proton donors (N–H) and two kinds of proton acceptors (carbonyl oxygen and ester oxygen) in MDI-based polyurethane. Figure 2 shows the optimized stable structures for hydrogen bonding of various conformers using B3LYP and B3PW91 methods. Structure (a) is a free molecule lacking any hydrogen

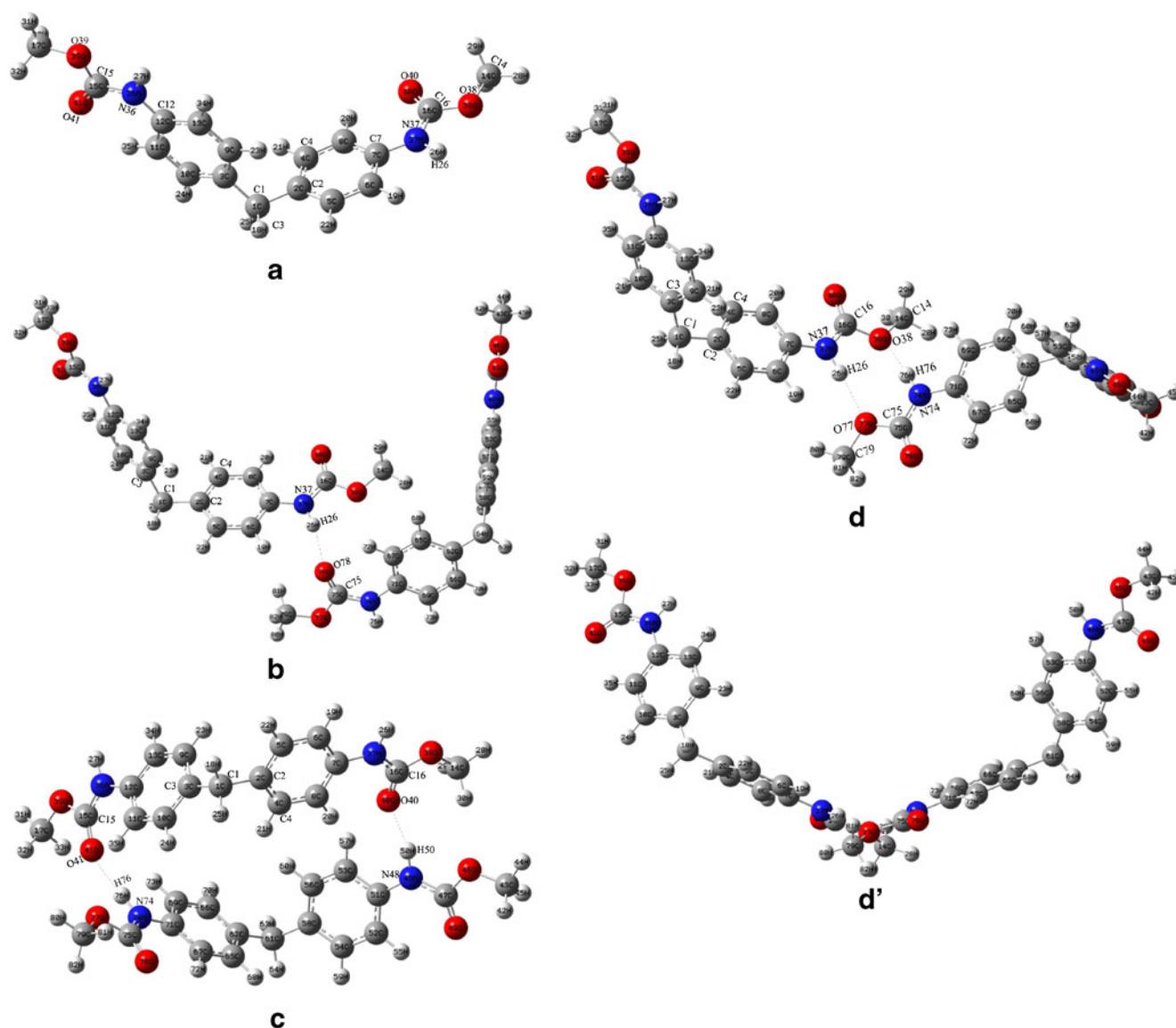


Fig. 2 Optimized structures for possible H-bonds. Structures (a), (b), (c), (d) and (d') are shown

Table 1 Selected intermolecular and intramolecular structure data (bond lengths in Angstroms, bond angles in degrees) for the optimized structures^a at both B3LYP/6–31G* and B3PW91/6–31G* levels

Structure	Parameter	B3LYP	B3PW91	R(N–H···O)
(a)	R(C15=O41)	1.216	1.214	
	R(C16=O40)	1.216	1.214	
	R(N37–H26)	1.011	1.010	
	R(C14–O38)	1.434	1.427	
	R(C16–O38)	1.363	1.358	
	θ (C3–C1–C2–C4)	–59.05	–57.68	
	θ (C7–N37–C16–O38)	180.0	–179.9	
	θ (C12–N36–C15–O39)	179.8	–179.8	
(b)	R(N37–H26)	1.017	1.016	2.89 [9, 21] and 3.15–3.16 [22]
	R(C75=O78)	1.224	1.219	
	R(N37–H26···O78)	3.028	3.020	
	θ (N37–H26···O78)	167.5	175.8	
	θ (C3–C1–C2–C4)	–55.85	–58.42	
(c)	R(C15=O41)	1.221	1.219	2.89 [9, 21] 3.15–3.16 [22]
	R(N74–H76)	1.017	1.017	
	R(N74–H76···O41)	3.012	3.025	
	θ (N74–H76···O41)	174.3	174.3	
	R(C16=O40)	1.223	1.220	
	R(N48–H50)	1.018	1.018	
	R(N48–H50···O40)	3.005	3.022	
	θ (N48–H50···O40)	166.8	167.6	
(d)	θ (C3–C1–C2–C4)	–63.0	–62.13	
	R(C14–O38)	1.438	1.431	2.99 [9] 3.15–3.16 [21]
	R(C16–O38)	1.378	1.372	
	R(N74–H76)	1.017	1.017	
	R(N74–H76···O38)	3.074	3.075	
	θ (N74–H76···O38)	173.1	171.7	
	R(C79–O77)	1.438	1.431	
	R(C75–O77)	1.378	1.372	
	R(N37–H26)	1.017	1.017	
	R(N37–H26···O77)	3.074	3.075	
	θ (N37–H26···O77)	173.1	171.7	
θ (C3–C1–C2–C4)	–58.54	–52.67		

^a Atom numbering is in accordance with Fig. 2

bonding, while complex (b) forms one H-bond between the carbonyl oxygen and the amidogen hydrogen. Complexes (c) and (d) both have two H-bonds, with the difference being the binding site with the amidogen hydrogen (the former is the carbonyl oxygen, the latter is the ester oxygen). Complex (d) is a profile of complex (c) after rotation in three-dimensional space.

Table 1 lists the DFT-calculated distances and angles of the intermolecular hydrogen bonds in MDI-based polyurethane. Analysis of hydrogen-bonded geometries in the calculated structures reveals that the B3LYP approximation results generally in slight longer covalent bonds (single and double bonds) and shorter hydrogen bonds [except for N37–H26···O78 in complex (b)] in comparison to the corresponding values of the B3PW91-optimized geometries.

The distances of R(N–H), R(C=O) and R(C–O) involved in hydrogen bonding are elongated to some degree in the forming of H-bonds with correspondingly stretched ratios of 0.6%, 0.4% and 0.7%, respectively. The H-bond distances for complexes (b) and (c) [R(N37–H26···O78), R(N74–H76···O41) and R(N48–H50···O40)] are comparable with the largest deviations found 0.029 Å by B3LYP and 0.016 Å by B3PW91, respectively. For complex (d), the H-bond distances are much longer than the others, with the smallest differences being 0.035 Å and 0.045 Å by B3LYP and B3PW91, respectively. These values indicate that the H-bond distance to the ester oxygen is longer than that to the carbonyl oxygen. The H-bond distances obtained are in excellent agreement with experimental values [9, 21, 22]. The angles related to the H-bond A(N–H···O) are all close to 180°, in

accordance with the measurable criteria for H-bonds [23]. The dihedral angle of the two planes D(C3–C1–C2–C4) in complex (c) is the largest among the four structures (a), (b), (c) and (d), which may be due to steric hindrance when two molecules close to each other form two H-bonds. The largest deviation of H-bond distances by the two methods for the same bond is 0.017 Å in H-bond (N48–H50···O40), while the largest difference in angles is 8.3° in the angle A(N37–H26···O78). Thus, we can see that the two methods give similar and reasonable results.

Mulliken charges

Table 2 shows the Mulliken charges on the key atoms of the interactions calculated by two methods; ΔQ is the change in the charges on the atoms due to hydrogen bonding. From the charge distribution of the four structures, we can see that nitrogen and oxygen atoms carry negative partial charge, while the hydrogen atoms bonded to them carry positive partial charge. The initial charges on O77, O78, N48, N74, H50 and H76 before hydrogen bonding are the same as those of O39, O41, N37, N36, H26 and H27 in structure (a), respectively, and are listed as part of this structure (see Table 2 for a comparison with the corresponding hydrogen bonded atoms).

The Mulliken charges calculated by B3LYP are slightly higher than those by B3PW91 for most atoms (Table 2). All atoms involved in hydrogen bonding exhibit some change in charge, and the variation tendency of nitrogen atoms and

oxygen atoms are more in the negative direction, while the hydrogen atoms bonded to them are more in the positive direction (see ΔQ column), due to a shift in electron density from hydrogen toward that of nitrogen and oxygen.

There is no direct relationship between the net charge ($\Delta Q_O + \Delta Q_N + \Delta Q_H$) for each hydrogen bond and the corresponding structure. For complexes (b) and (c), the net charges are 0.003 (N37–H26···O78), 0.006 (N74–H76···O41) and 0.007 (N48–H50···O40) by B3LYP; all are close to zero, indicating that the charge is transferred mainly among the N, H and O atoms involved in hydrogen bonding. For complex (d), the net charges are –0.036 (N74–H76···O38) and –0.045 (N37–H26···O77) by B3LYP. Both net charges have a considerable negative value, which means the adjacent atoms of the hydrogen-bonding atoms are also involved in charge transfer. By the B3PW91 method, the net charges are 0.027 (N37–H26···O78) for complex (b), 0.016 (N74–H76···O41) and 0.002 (N48–H50···O40) for complex (c), –0.009 (N74–H76···O38) and –0.010 (N37–H26···O77) for complex (d). The net charges for the three complexes differ to some degree by two methods, but the charge transfer is validated nonetheless. Hence, intermolecular charge transfer dominates the charge rearrangement in all complexes as H-bonds are formed.

Thermal parameters of hydrogen bonding

In order to show the relationship between stability and hydrogen bonds, the relative binding energies ΔE ,

Table 2 Predicted Mulliken charges on key points of the interactions

Atom	B3LYP				ΔQ^e	B3PW91				ΔQ^e
	Structure					Structure				
	(a)	(b)	(c)	(d)		(a)	(b)	(c)	(d)	
O38	–0.462	–	–	–0.548	–0.086	–0.499	–	–	–0.519	–0.020
O39	–0.465	–	–	–	–	–0.498	–	–	–	–
O40	–0.505	–	–0.511	–	–0.006	–0.509	–	–0.527	–	–0.018
O41	–0.504	–	–0.523	–	–0.019	–0.510	–	–0.526	–	–0.016
O77	–0.465	–	–	–0.548	–0.083	–0.498	–	–	–0.519	–0.021
O78	–0.504	–0.522	–	–	–0.018	–0.510	–0.517	–	–	–0.007
N36	–0.743	–	–	–	–	–0.788	–	–	–	–
N37	–0.727	<i>–0.779</i>	–	–0.777	<i>–0.052/–0.050</i>	–0.788	<i>–0.838</i>	–	–0.824	<i>–0.050/–0.036</i>
N48	–0.727	–	–0.780	–	–0.053	–0.788	–	–0.818	–	–0.030
N74	–0.743	–	<i>–0.763</i>	–0.777	<i>–0.020/–0.034</i>	–0.788	–	<i>–0.825</i>	–0.824	<i>–0.037/–0.036</i>
H26	0.331	<i>0.398</i>	–	0.419	<i>0.067/0.088</i>	0.365	<i>0.449</i>	–	0.412	<i>0.084/0.047</i>
H27	0.335	–	–	–	–	0.366	–	–	–	–
H50	0.331	–	0.397	–	0.066	0.365	–	0.419	–	0.054
H76	0.335	–	<i>0.380</i>	0.419	<i>0.045/0.084</i>	0.365	–	<i>0.434</i>	0.412	<i>0.069/0.047</i>

^e In cases where the same atom is involved in hydrogen bonding in two complexes, one complex is indicated in italics and the other in normal typeface

Table 3 Binding energies ΔE (kJ mol^{-1}), $\Delta E_{\text{BSSE+ZPE}}^{\text{a}}$ (kJ mol^{-1}) and binding enthalpy ΔH (kJ mol^{-1}) for the H-bonds of various complexes

Structure	Method	ΔE	BSSE	ZPE	$\Delta E_{\text{BSSE+ZPE}}^{\text{a}}$	ΔH	Reference
(b)	B3LYP	-25.60	14.39	-0.11	-11.32	-22.84	31.38 [9] for ΔH
	B3PW91	-18.67	8.63	-0.10	-10.14	-15.09	
(c)	B3LYP	-48.21	23.82	-0.24	-24.63	-46.88	
	B3PW91	-35.70	18.69	-0.24	-17.25	-34.12	
(d)	B3LYP	-24.66	12.58	-0.16	-12.24	-22.02	
	B3PW91	-17.65	10.43	-0.14	-7.36	-14.86	

^a Corrected by basis set superposition error (BSSE) and zero-point vibrational energy (ZPE)

$\Delta E_{\text{BSSE+ZPE}}$ (including the BSSE and ZPE corrections) and the binding enthalpies ΔH , for the three complexes [(b), (c) and (d)] were calculated by the two methods (see Table 3).

The differences in binding energies and enthalpies for the same complex according to the two methods are considerable, reaching $12.76 \text{ kJ mol}^{-1}$ for complex (c) in binding enthalpy. Comparing the binding energies ($\Delta E_{\text{BSSE+ZPE}}$) of the three complexes, the data calculated by the B3LYP method were found to be higher than that calculated by the B3PW91 method, with the biggest difference being 7.38 kJ mol^{-1} for complex (c). For the same method, the binding energies ($\Delta E_{\text{BSSE+ZPE}}$) of complexes (b) and (d) are close to each other, and are almost half of that of complex (c) by the corresponding method. From Fig. 2, we can see that complex (b) has only one carbonyl bonded H-bond, and complex (c) contains two carbonyl-bonded H-bonds, while complex (d) includes two ester oxygen H-bonds. This indicates that the hard–soft segments are more weakly hydrogen-bonded than the hard–hard segments [22], which may be the reason for the phase separation and phase mixing in the polyurethanes.

Comparing the binding enthalpies for the three complexes by both methods to that reported in the literature [9], the binding enthalpy of complex (c) by the B3PW91 method is closest, with 5.8% difference. This indicates that the hydrogen binding pattern of complex (c), which contains two carbonyl bonded H-bonds, dominates in polyurethane, which means that most of the carbonyl oxygens in polyurethane exists in the hydrogen-bonded form, and that the B3PW91 method yields better data when modeling H-bond enthalpy.

In the case of complex (c), the BSSE corrections are 49.4% (B3LYP), and 52.4% (B3PW91) of the uncorrected ΔE , where the proportions of ZPE to the uncorrected ΔE are 0.6% (B3LYP) and 0.7% (B3PW91), respectively. This indicates that BSSE correction is necessary for calculating H-binding energies using these two methods, while the effect of ZPE correction is slight, and need not be taken into account.

Dipole moments

Many molecules have dipole moments due to non-uniform distributions of positive and negative charges on the various atoms. A molecule is polarized when it carries an induced

dipole, which occurs when one molecule with a permanent dipole repels another molecule's electrons, "inducing" a dipole moment in that molecule. One of the more important properties of hydrogen-bonded complexes is the electric dipole moment. The dipole moments for the four structures (see Fig. 2), i.e., the isolated molecular complex (a) and three hydrogen bonded complexes [(b), (c) and (d)] calculated by the two methods are listed in Table 4.

Comparing the values, the two methods produce similar dipole moments for the corresponding structures, within 0.4 D. For complex (b), the dipole moment is slightly higher than that of the isolated monomer but lower than simple vector addition of those of two isolated monomers, which may be due to partial dipole compensation from the additional hydrogen bond. Complex (c) features the largest dipole moment, which increases by almost twice relative to the isolated molecular complex, with an induced dipole moment of nearly 2.30 D by both methods due to the stronger interaction with the electron. Complex (d) has the smallest dipole moment, lower than that of the isolated monomer, which may be caused by the symmetry of the two monomers [see (d') in Fig. 2]; most of the dipoles tend to cancel out each other almost completely.

The dipole moment of an interacting pair of molecules differs from the vector sum of the permanent dipoles of the monomers because each molecule is polarized by the nonuniform electric field of its partner, which depends slightly on the geometry of the complex.

IR spectra

IR spectra were obtained through frequency calculation of different structures (see Fig. 3). Spectra a, b, c and d were calculated by the B3LYP method, while a', b', c' and d' were calculated by the B3PW91 method. Four spectral regions are of main interest in this study: two kinds of N–H stretching vibration from $3,150$ to $3,600 \text{ cm}^{-1}$, the carbonyl (C=O) stretching vibration from $1,600$ to $1,800 \text{ cm}^{-1}$, as well as the ester (C–O–C) stretching vibration from $1,000$ to $1,300 \text{ cm}^{-1}$.

Analysis of the N–H stretching absorption data is complicated due to the presence of two types of hydrogen bonds: N–H \cdots O=C (carbonyl bonded in hard segment) and

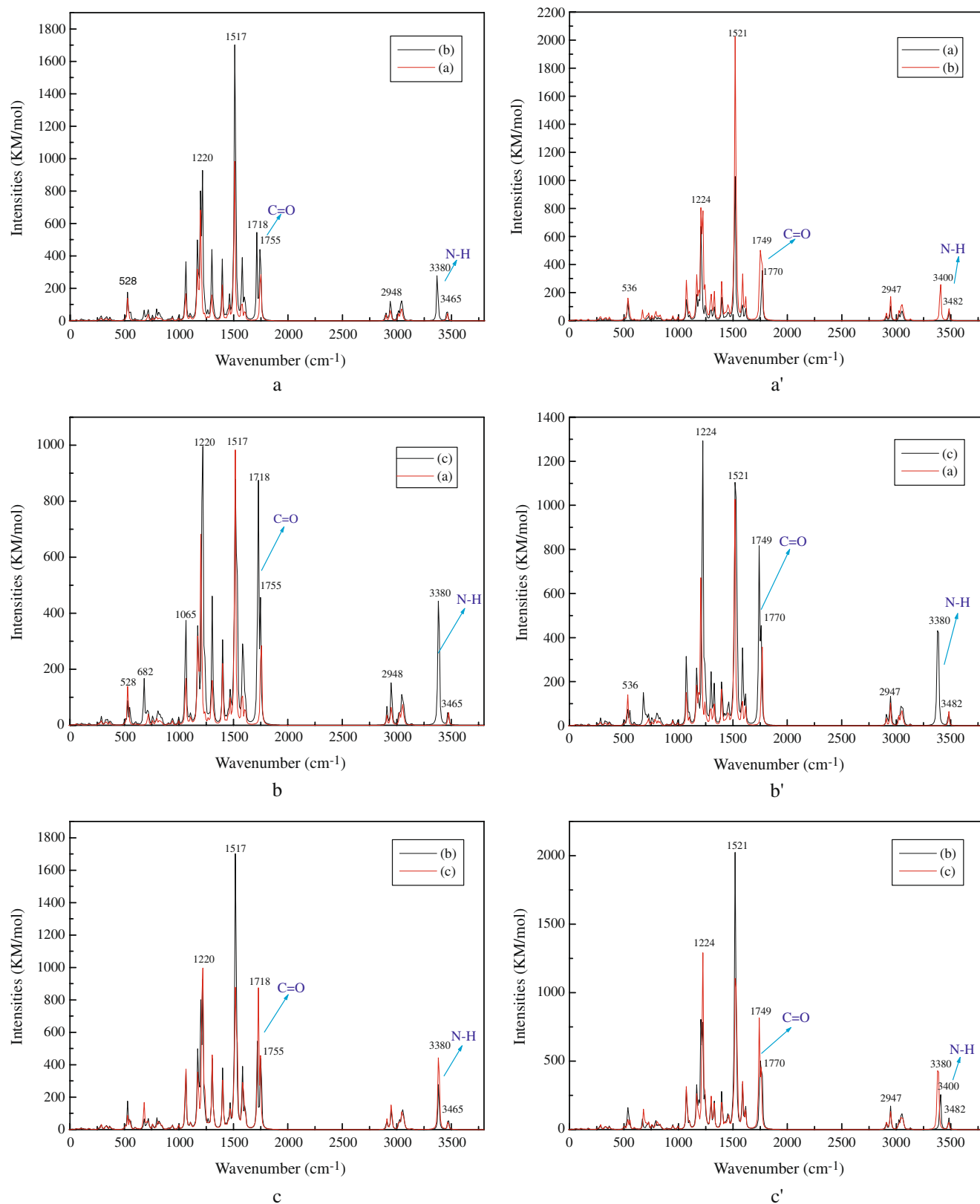


Fig. 3 Infrared (IR) spectra for the hydrogen bonding structures (a), (b), (c) and (d)

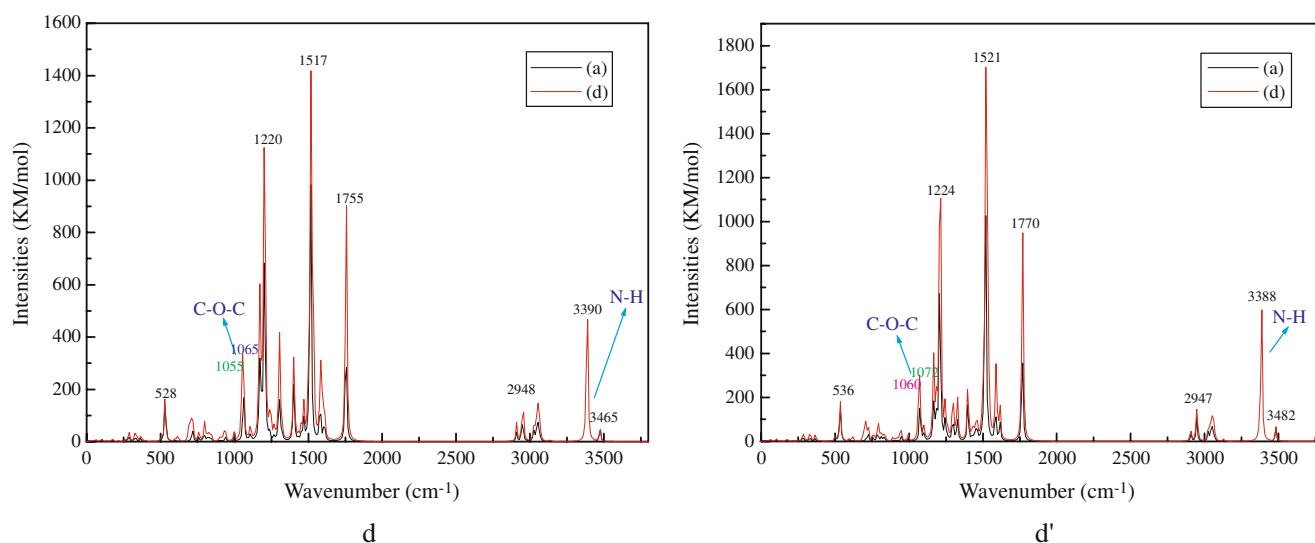


Fig. 3 (continued)

N–H···O (ester bonded in soft segment). Furthermore, there is disagreement over the frequency and absorptivity coefficient of the N–H stretching vibration for the N–H group hydrogen bonded to the ester oxygen [6, 8, 10, 11].

Looking at spectra a, b, c and d in Fig. 3, we find that the N–H stretching vibration exhibits two strong absorption peaks centered at around 3,380 cm^{-1} (a, b, c; 3,330 cm^{-1} in [9], 3,315 cm^{-1} in [22], 3,289 cm^{-1} in [25]) and 3,390 cm^{-1} (d; 3,295 cm^{-1} in [11], 3,268 cm^{-1} in [22], 3,270 cm^{-1} in [25]) arising from the hydrogen bonding of N–H to carbonyl groups and ester oxygen, respectively. The free N–H stretching vibration appears as a weak shoulder at about 3,465 cm^{-1} (3,420 cm^{-1} in [9], 3,445 cm^{-1} in [22], 3,480 cm^{-1} in [25]), and the frequency shift is nearly 85 cm^{-1} for the carbonyl H-bonding N–H and 75 cm^{-1} for the ester H-bonding N–H, respectively. This indicates that the strength of the carbonyl bonded H-bond is higher than that of the ester bonded H-bond.

The hydrogen-bonded carbonyls are formed by inter-urethane hydrogen bonding resulting from self-association, while most free carbonyls are formed when hard-segment and soft-segment mixing occurs, thereby giving rise to hydrogen bonding between urethane and ester groups [6–8, 12, 24].

The spectra a, b and c in Fig. 3 for the IR comparison of structure (a), complex (b) and (c) appear to be composed of two bands at the polyurethane carbonyl stretching region. The narrower band centered at around 1,755 cm^{-1} (1,735 cm^{-1} in [9], 1,729 cm^{-1} in [22], 1,729–1739 cm^{-1} in [25]) is assigned to the stretching of free carbonyl groups, while the band at 1,718 cm^{-1} (1,703 cm^{-1} in [9], 1,710 cm^{-1} in [22], 1,706–1,713 cm^{-1} in [25]) is attributed to the hydrogen-bonded carbonyl groups, and the frequency shift is nearly 40 cm^{-1} .

From the IR spectrum in Fig. 3 comparing structure (a) and complex (d), we can see that there is an obscure shift at around 1,060 cm^{-1} ; the 1,065 cm^{-1} (1,080 cm^{-1} in [9], 1,110 cm^{-1} in [25]) component can be assigned to the ester oxygen free of hydrogen bonding, and the lower frequency component at 1,055 cm^{-1} is associated with the hydrogen-bonded ester oxygen, and the frequency shift is only 17 cm^{-1} , which is less than that of the carbonyl group. This also indicates hard–hard segment H-bonding is stronger than that of hard–soft segments.

A similar frequency shift trend was also observed by the B3PW91 method (see a', b', c', d' in Fig. 3). In each spectrum, the strong absorption peak centered around 3,380 cm^{-1} can be assigned to the hydrogen-bonded N–H groups by carbonyl, and another strong absorption peak centered around 3,388 cm^{-1} is assigned to the hydrogen-bonded N–H groups by the ester oxygen, while the weak shoulder on the high-frequency side of these peaks corresponds to free N–H groups. The narrower band centered at around 1,770 cm^{-1} is assigned to the stretching of free urethane carbonyl groups, while the band at 1,749 cm^{-1} is attributed to hydrogen-bonded urethane

Table 4 Dipole moment (in Debye) of the various structures calculated by two methods

Method	Structure			
	(a)	(b)	(c)	(d)
B3LYP	3.5711	4.5696	9.4018	2.4453
B3PW91	3.5590	4.9437	9.4851	2.3968

carbonyl groups. An obscure shift at around $1,060\text{ cm}^{-1}$ can be found, the $1,072\text{ cm}^{-1}$ component is assignable to the ester oxygen free of hydrogen bonding, and the lower frequency component at $1,060\text{ cm}^{-1}$ is associated with the hydrogen-bonded ester oxygen.

Most of the spectra for complexes (b) and (c) (see c or c' in Fig. 3) coincide very well in terms of frequency (with the exception of some differences in the vibration of N–H bonded by H-bond with the B3PW91 method), but differ in intensity at frequencies $\nu=3,380\text{ cm}^{-1}$, $1,718\text{ cm}^{-1}$ and $1,517\text{ cm}^{-1}$ by B3LYP ($\nu=3,380\text{ cm}^{-1}$, $1,749\text{ cm}^{-1}$ and $1,521\text{ cm}^{-1}$ by B3PW91), which refer to the vibration of ν (N–H) hydrogen-bonded, C=O hydrogen-bonded urethane carbonyl, and δ (N–H) + ν (C–N) [9, 25] aroused by the different number of H-bonds.

The IR spectrum data calculated by the two methods are very close to each other within 30 cm^{-1} , while the B3LYP method predicts better vibrational frequencies compared to the experimental spectra. The appearance of new bands at the lower frequency side of free N–H, C=O and C–O–C absorption is evidence for the formation of hydrogen bonds. The frequency shift for carbonyl H-bonding is bigger than that of ester H-bonding, which means the former is stronger. Thus, the H-bonding trend can be easily forecast from IR using theoretical methods.

Conclusions

The hydrogen-bonding properties of hard–hard and hard–soft segments in MDI-based polyurethane were investigated by DFT methods. The structures, Mulliken charges, dipole moments, binding energies, binding enthalpies, and IR spectra were obtained using both B3LYP and B3PW91 methods. The bond distances calculated by both methods were in the range of $3.005\text{--}3.028\text{ \AA}$ for the carbonyl bonded H-bond and $3.074\text{--}3.075\text{ \AA}$ for the ester bonded H-bond, and were in reasonable agreement with experimental values. Charge transfer on the N, H and O atoms involved in hydrogen bonding occurs upon the formation of H-bonds. Most of the carbonyl oxygen in polyurethane exists in the hydrogen-bonded form, and the B3PW91 method gives better results when modeling H-bonding enthalpy. Intermolecular charge transfer dominates the charge rearrangement in all complexes as H-bonds are formed. The dipole moment of an interacting pair of molecules differs from the vector sum of the permanent dipoles of the monomers, and depends slightly on the geometry of the complex. The appearance of new bands at frequencies lower than those of free N–H, C=O and C–O–C absorption is evidence for the formation of H-bonds, which can be easily forecast by theoretical methods. In addition, the hard–soft segments are more weakly hydrogen-bonded than the hard–hard segments.

The theoretical methods used here are helpful tools in predicting and confirming the properties of these materials, and will be useful in the future design of new materials.

Acknowledgment This work was financially supported by the project “Development of Shape Memory Knitted Fabrics/Garments” (K.14.37.ZR01). The authors wish to express their gratitude for this generous support.

References

- Lendlein A, Kelch S (2002) *Angew Chem Int Ed* 41:2034–2057
- Lee BS, Chun BC, Chung YC, Sul KI, Cho JW (2001) *Macromolecules* 34:6431–6437
- Lai YC, Quinn ET (1995) *J Polym Sci A* 33(11):1767–1772
- Takahashi T, Hayashi N, Hayashi S (1996) *J Appl Polym Sci* 60:1061–1069
- Yang JH, Chun BC, Chung YC, Cho JH (2003) *Polymer* 44:3251–3258
- Coleman MM, Skrovanek DJ, Hu J, Painter PC (1988) *Macromolecules* 21:59–65
- Srichatrapimuk VW, Cooper SL (1978) *J Macromol Sci Phys* 15:267–311
- Senich GA, MacKnight WJ (1980) *Macromolecules* 13:106–110
- Brunette CM, Hsu SL, MacKnight WJ (1982) *Macromolecules* 15:71–77
- Christenson CP, Harthcock MA, Meadows MD, Spell HL, Howard WL, Creswick MW, Guerra RE, Turner RBP (1986) *J Polym Sci B* 24:1401–1439
- Lee HS, Wang YK, Hsu SL (1987) *Macromolecules* 20:2089–2095
- Lee SS, Wang YK, MacKnight WI, Hsu SL (1988) *Macromolecules* 21(1):270–273
- Hadzi D (ed) (1997) *Theoretical treatment of hydrogen bonding*. Wiley, Chichester
- Bene JED (1998) *Hydrogen bonding 1: encyclopedia of computational chemistry*, vol 2. Wiley, New York
- Becke AD (1993) *J Chem Phys* 98:5648–5652
- Becke AD (1988) *Phys Rev A* 38:3098–3100
- Lee WYC, Parr RG (1988) *Phys Rev B* 37:785–789
- Perdew JP, Chevary JA, Vosko SH, Jackson KA, Pederson MR, Singh DJ, Fiolhais C (1992) *Phys Rev B* 46:6671–6681
- Boys SF, Bernardi F (1970) *Mol Phys* 19:553–566
- Frisch MJ, Trucks GW, Schlegel HB, Scuseria GE, Robb MA, Cheeseman JR, Zakrzewski VG, Montgomery JA Jr, Stratmann RE, Burant JC, Dapprich S, Millam JM, Daniels AD, Kudin KN, Strain MC, Farkas O, Tomasi J, Barone V, Cossi M, Cammi R, Mennucci B, Pomelli C, Adamo C, Clifford S, Ochterski J, Petersson GA, Ayala PY, Cui Q, Morokuma K, Malick DK, Rabuck AD, Raghavachari K, Foresman JB, Cioslowski J, Ortiz JV, Stefanov BB, Liu G, Liashenko A, Piskorz P, Komaromi I, Gomperts R, Martin RL, Fox DJ, Keith T, Al-Laham MA, Peng CY, Nanayakkara A, Gonzalez C, Challacombe M, Gill PMW, Johnson BG, Chen W, Wong MW, Andres JL, Head-Gordon M, Replogle ES, Pople JA (2003) *Gaussian 2003W Revision B.05*. Gaussian Inc, Pittsburgh
- Lord RC, Merrifield RE (1953) *J Chem Phys* 21:166–167
- Teo LS, Chen CY, Kuo JF (1997) *Macromolecules* 30(6):1793–1799
- Vergenz RA, Yazji I, Whittington C, Daw J, Tran KT (2003) *J Am Chem Soc* 125:12318–12327
- Hwang KKS, Wu G, Lin SB, Cooper SL (1984) *J Polym Sci Polym Chem Ed* 22(7):1677–1697
- Luo N, Wang DN, Ying SK (1997) *Macromolecules* 30(15):4405–4409